Chalcogenide Letters Vol. 22, No. 10, October 2025, p. 863 - 870

Role of engineered Co_4S_3 and Ce_2S_3-Co_4S_3 binary composite materials for clean and high-performance energy solutions

M. Danish [a] , Z. A. Sandhu [b], S. Sajid [a], S. R. Shafqat [a], R. Abbas [c], M. Shahid [d], N. Amjed [e], A. Abo Elnasr [f], H. T. Ali [f], M. A. Raza [b, *]
[a] *Department of Chemistry, Faculty of Science, University of Sialkot, Sialkot, 51310, Pakistan*
[b] *Department of Chemistry, Faculty of Science, University of Gujrat, Hafiz Hayat Campus, Gujrat, 50700, Pakistan*
[c] *Department of Chemistry, Division of Science and Technology, University of Education, Lahore, 54000, Lahore, Pakistan.*
[d] *Interdisciplinary Research Center in Biomedical Materials (IRCBM), COMSATS University Islamabad, Lahore Campus, Lahore 54000, Punjab, Pakistan*
[e] *Department of Chemistry, University of Lahore, Lahore, Pakistan*
[f] *Department of Mechanical Engineering, College of Engineering, Taif University, Kingdom of Saudi Arabia*

The increase in energy crisis and environmental concerns are now considering as major hurdle in way to sustainability and clean energy solution. Metal sulfides have been investigated for the fabrication of energy conversion ad storage devices to overcome the effect of energy demand. In this concern, a microemulsion mediated hydrothermal method was employed for the successful synthesis of pure Co_4S_3 and Ce_2S_3-Co_4S_3 binary nanocomposite materials. This study was investigated for Supercapacitor application using cyclic voltammetry and electrochemical impedance spectroscopy. The scanning electron microscope analysis of composite material showed compact smooth morphology with strong interparticle interactions. The cyclic voltammetry was assessed for the determination of specific capacitance and energy density of material. The Ce_2S_3-Co_4S_3 binary nanocomposite demonstrated excellent specific capacitance and energy density value of 952 F/g and 33.06 Wh/kg, respectively. The higher capacitance and energy density value of Ce_2S_3-Co_4S_3 binary nanocomposite is due to its strong synergistic interaction between both metals. Similarly, the electrochemical impedance spectroscopy demonstrated the effective kinetic behavior of Ce_2S_3-Co_4S_3 binary nanocomposite. This recommends composite material a strong candidate in class of metal sulfide for greener sustainable solutions.

(Received July 21, 2025; Accepted October 6, 2025)

Keywords: Energy solution, Binary composites, Metal sulfides

1. Introduction

The major increase in industrialization processes and change in energy sources has always been brings difficult for sustainable economic growth [1]. The rise in the growth of global transportation and energy infrastructure, increasing energy consumption and play vital role in the degradation of environment. Researchers are focusing on clean and high-performance energy solutions [2]. The world is transferring its activities towards renewable and efficient energy sources by developing large capacity energy storage devices and systems [3]. The development of advance energy storage devices like batteries, fuel cell and Supercapacitor are the most appropriate solution to meet the current energy crisis and environmental deterioration [4]. These devices are mainly required to charge mobile devices, hybrid and electric cars, renewable power networks, and other industrial infrastructures [5]. Among all electrochemical energy storage systems, Supercapacitor are mainly focused sue to its distinct advantages like high energy density, power density and charge storage capacity [6, 7].

* Corresponding authors: asamgcu@yahoo.com
https://doi.org/10.15251/CL.2025.2210.863

The Supercapacitor have been divided into three types, electrochemical double-layer capacitors (EDLCs), pseudocapacitors and hybrid capacitors [8]. The EDLCs based on the phenomenon of electrostatic charge at the interface of electrode-electrolyte, and pseudocapacitors involves fast and reversible Faradaic redox reactions [9]. In spite of various advantages, Supercapacitor continue to have concerns in rate capability. To overcome these hurdles in energy storage system, the researchers make efforts on the development of new metal sulfide electrode materials with large surface area, improved conductivity and redox reactions [10]. Transition metal sulfides (TMSs) are considering advanced active electrode materials for next-generation Supercapacitor. They are better than conventional electrode materials owing to their high electrical conductivity, redox-friendly, and structural controllability [11]. TMSs like molybdenum sulfide, vanadium sulfide, nickel sulfide, and cobalt sulfide have shown excellent pseudocapacitive performance [12, 13]. TMSs nanomaterials have been synthesized via various synthetic approaches, includes, co-precipitation, sol-gel, chemical vapor deposition, hydrothermal, and solvothermal process [14]. In all these synthetic processes, a microemulsion-mediated hydrothermal approach is distinguished due to its efficiency in achieving control particle size, shape and homogeneity under mild thermodynamic conditions. The approach allows homogenous nanostructured with very high surface area and porosity, facilitating fast ions transportation and redox interaction on electrodes [15].

Cobalt sulfide has been considered as valuable 3d-transition metal, ability to show multiple oxidation states, high theoretical capacitance and suitable electronic properties. It is found in several crystalline form, like CoS, CoS_2 and Co_4S_3 and has extensive redox chemistry [16]. Similarly, cerium sulfide (Ce_2S_3) chemically stable and involves reversible process by oxidation reduction in Ce^{3+}/Ce^{4+} [17]. Research on Ce/$CoNi_2S_4$ nanocomposites for Supercapacitor has been reported by Wang, et al., (2021). The pure $CoNi_2S_4$ electrode demonstrated specific capacitance of 1988 F/g at 1 A /g, but the Ce/$CoNi_2S_4$ electrode showed capacitance of 2408 F/g [18]. This research work intends to synthesize Ce_2S_3-Co_4S_3 binary nanocomposites via microemulsion-assisted hydrothermal technique and assess the electrochemical properties of prepared nanomaterials for Supercapacitor application. The resulting Ce_2S_3-Co_4S_3 shows significant Supercapacitor performance due to strong synergistic effect of cerium in cobalt lead to increase active sites, better diffusion of ions and improved cycling stability.

2. Experimental work

2.1. Synthesis of pure Co_4S_3 and Ce_2S_3-Co_4S_3 binary nanocomposite

The Pure Co_4S_3 and Ce_2S_3-Co_4S_3 binary composite was prepared with modified micro-emulsion mediated hydrothermal approach [13, 19]. The oil-emulsion was prepared using cyclohexane, TX-100, and n-butanol as solvent, surfactant and co-surfactant, respectively. On the other hand, cobalt (III) chloride ($CoCl_2$), and cerium Sulphate $Ce(SO_4)_2$ was dissolved in water to prepare water emulsion. The water emulsion was introduced into oil-emulsion to form water/oil micro-emulsion. A calculated amount of ammonium sulphate was added in above micro-emulsion as a Sulphur source. Later, the solution was transferred into autoclave for specific heat treatment at 150 ˚C for 20 h. After this process, the autoclave was allowing to cool down and then performed washing of material. The above solution was washed with ethanol and deionized water. The washed particles were later dried at 100-150˚C. Finally, a fine power was obtained as composite material. The pure nanomaterial was prepared with same procedure with a minor change in water emulsion. The water emulsion contains only sing meta precursor salt.

3. Results and discussion

3.1. Characterization

The Fourier transform infrared spectroscopy (FTIR) was performed for the determination of functional group and vibrational motions. The stretching vibrations of OH group correspond to a notable peak at 3216 cm^{-1} [20, 21]. The absorption range from 1729-1511 cm^{-1} is may be due to bending and stretching vibrations of OH group. The presence of sharp peaks at 857 cm^{-1} and 600

cm^{-1} indicates vibrations of metal -sulfur bonds (Ce-S and Co-S) [22-24], which confirms the general formation of the metal sulfide phase in composite material. The band at 1050 cm^{-1} can be assigned to symmetric stretching vibration of sulfate/sulfur-oxygen (Co-S), a shared common phase of pure and the composite material [25]. The existence of this common vibrational zone ensures the structural association of Co_4S_3 with Ce_2S_3 nanocomposite. Figure 1 illustrated about FTIR analysis of pure and composite material.

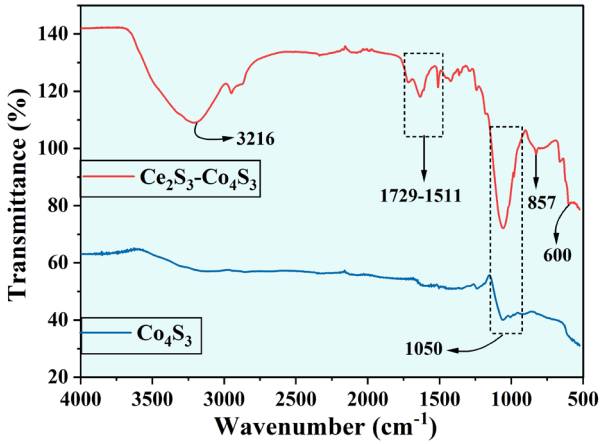

Fig. 1. FTIR Spectra of synthesized nanoparticles (a) Co_4S_3 pure phase (b) Ce_2S_3-Co_4S_3 binary composites.

The composition and structure of synthesized nanoparticles were determined by X-ray diffraction spectroscopy (XRD) analysis. The XRD pattern of pure Co_4S_3 and Ce_2S_3- Co_4S_3 composite are shown in figure 2. The observed peaks are indexed to the standard JCPDS cards. The main diffraction peaks are observed at 2θ values of about 24°, 29°, 33°, 41°, 45°, 49°, and 52°, which presented the (211), (220), (310), (400), (420), (332), (422) planes are attributed to the orthorhombic form of Ce_2S_3 with JCPDS card # 00-027-0104 [13, 26, 27]. Other peaks appearing at the 2θ positions of 20° (210), 22° (212), 30° (005), and 34° (231) are in agreement with the cubic phase of Ce_2S_3 (JCPDS # 00-020-0269) [24]. These peaks represent the secondary phase of Ce_2S_3. The incomplete reaction or phase segregation during the reaction may be considered to cause the existence of the secondary phase in the Ce_2S_3- Co_4S_3 composite. Moreover, the peaks at 2θ value 28.3° (311), 36.5° (400), and 39° (331) indicate phase of cobalt sulfide which corresponding to JCPDS card # 00-002-1338 [28]. This shows a confirmation of its integration in the composite. These peaks are highlighted as sharp and clear, which makes the composite prove to be crystalline. The appearance of these peaks which belong to several JCPDS patterns confirms the successful synthesis of a composite Ce_2S_3- Co_4S_3 with secondary cobalt sulfide phase embedded in the composite.

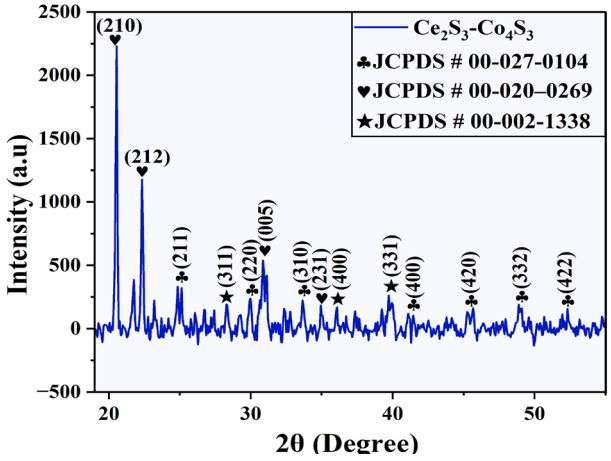

Fig. 2. XRD spectrum of synthesized Ce_2S_3-Co_4S_3 binary composites.

The scanning electron microscope (SEM) analysis was performed for the determination of morphology and structural changes in Co_4S_3 and Ce_2S_3-Co_4S_3 binary composite materials as shown in figure 3 (a, b). The SEM analysis presented different morphology and structural changes that directly influence on the electrochemical excellence of pure and composite nanomaterial. The pure Co_4S_3 demonstrated small particles with relatively scatter and lose aggregation that led to lower interconnectivity and limited packing density. Conversely, the Ce_2S_3-Co_4S_3 binary composite shows more refined, compact and larger particles structural morphology. This strongly packed structure ensures the improved particle contact. Improving charge kinetics. The cerium incorporation enhanced integrity of surface and surface roughness, that increase the active surface area and ion diffusion. This structural morphology recommends Ce_2S_3-Co_4S_3 binary material for Supercapacitor application.

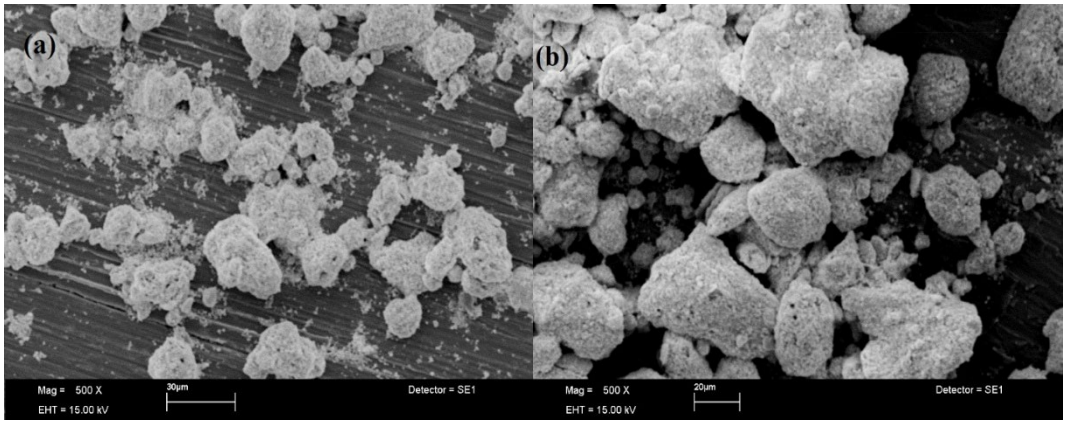

Fig. 3. SEM analysis of prepared nanomaterials, (a) pure Co_4S_3, and (b) Ce_2S_3-Co_4S_3 binary nanocomposite.

3.2. Electrochemical performance

The electrochemical excellence particularly in Supercapacitor performance was investigated via three electrode setups. The three-electrode setup was consisted of working electrode (Nickel foam), reference electrode (Ag/AgCl) and counter electrode (Pt wire). The Supercapacitor performance was determined in an electrolyte solution of 2M KOH. This molarity of KOH allow rapid faradic redox reactions. The cyclic voltammetry analysis was used to determine the redox reaction and capacitive behavior of prepared materials. The CV analysis was carried out at varying scan rates of 10 to 100mV/s with a capacity of increasing scan arte with 10 values after each run.

The CV curves showed distinctive characteristics of prepared material, like a minor rise in cathodic peak and simultaneously dropped in the anodic peak to lower voltage, representing the higher electrochemical reversibility of electrode material. These redox peaks in CV voltammogram may be corresponding to faraday redox reactions [29].

On the other hand, with the increase of scan rate a direct effect on area under the CV curve was observed. The increase in scan arte increases the area and showed a negative impact in its kinetic mechanism and capacitive behavior. The rise in scan rate involved, the reduction peak shifted to positive potential and correspondingly reduction peak towards negative potential values [30]. The CV analysis of pure Co_4S_3 and Ce_2S_3-Co_4S_3 depicted distinct redox efficiency and transportation of electron followed by ions diffusion. The specific capacitance and scan rate in the CV performance demonstrated inverse relationship with each other [31]. The Co_4S_3 electrode material showed restricted ion diffusion and kinetic mechanism that led to lower active sites and decline in surface area. This is may be due to low accessibility of electrolyte on the surface of electrode. The CV analysis of pure Co_4S_3 and Ce_2S_3-Co_4S_3 is depicted in figure 4.

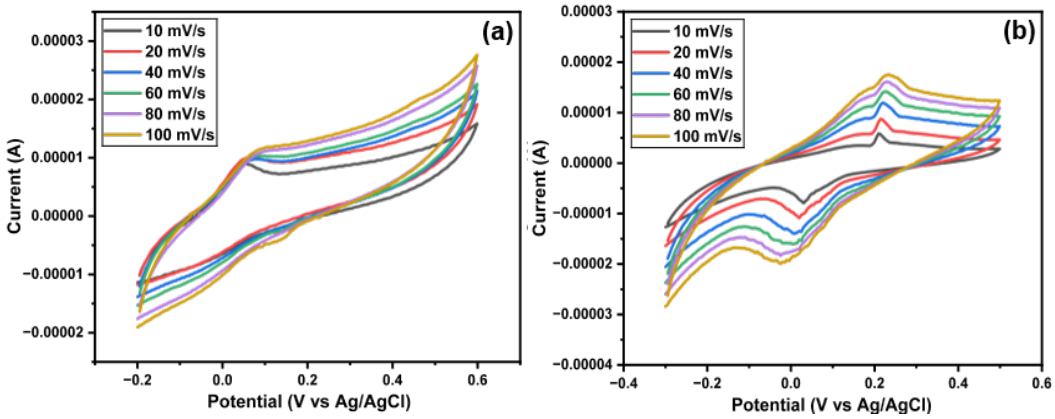

Fig. 4. Cyclic voltammetry and cyclic stability analysis of pure and composite materials, (a) CV curves of pure Co_4S_3, (b) CV curves of Ce_2S_3-Co_4S_3 composite material.

The Co_4S_3 and Ce_2S_3-Co_4S_3 binary composite material showed remarkable specific capacitance and energy density values due to enhanced surface area and improved active sites for ion diffusion. The specific capacitance of Co_4S_3 and Ce_2S_3-Co_4S_3 binary composite was 629 and 952 F/g, respectively at 10 mV/s. Similarly, the energy density value was calculated 21.83 and 33.06 Wh/kg, respectively. The higher specific capacitance and energy density value of Ce_2S_3-Co_4S_3 binary composite may be attributed to strong redox reaction and synergistic effect of cerium in Cobalt metal, improving active sites on the surface of electrode material. The specific capacitance and energy density comparisons is shown in figure 5.

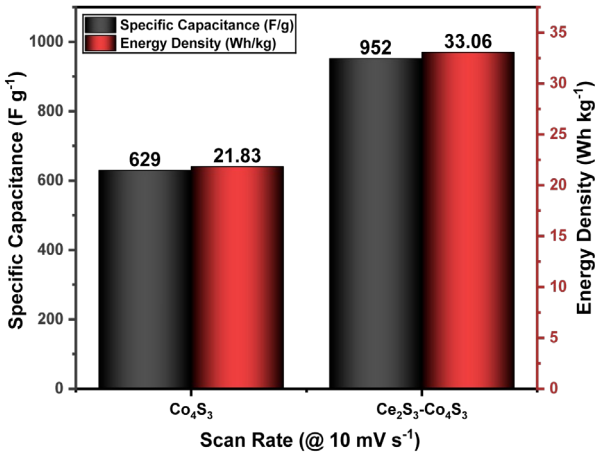

Fig. 5. Specific capacitance and energy density comparison of Co_4S_3 and Ce_2S_3-Co_4S_3 binary composite.

The electrochemical impedance spectroscopy was used for the determination of reaction kinetic and capacitive characteristics of Co_4S_3 and Ce_2S_3-Co_4S_3 binary composite. The EIS analysis was categorized into two segments, a semicircle and a straight line in a Nyquist plot. The semicircle in Nyquist plot provide information about the electrode-electrolyte resistance and ion diffusion at their interphase may attributed to conductivity of ions [32]. The higher semicircle demonstrated higher resistance between the electrolyte and electrode that lead to lower conductivity and slower ions transportation. Similarly, the pure Co_4S_3 showed higher semicircle than binary composite material exhibited less efficient electrode than composite material. Conversely, the Ce_2S_3-Co_4S_3 binary composite showed lower semicircle and improved ions conductivity and fast faradic redox reaction kinetics. The circuit in the EIS showed different types of resistance, solution resistance, charge and electrolyte transfer resistance. These resistances play pivot role in the electrochemical kinetics of electrode materials. Figure 6 showed the EIS analysis of prepared materials.

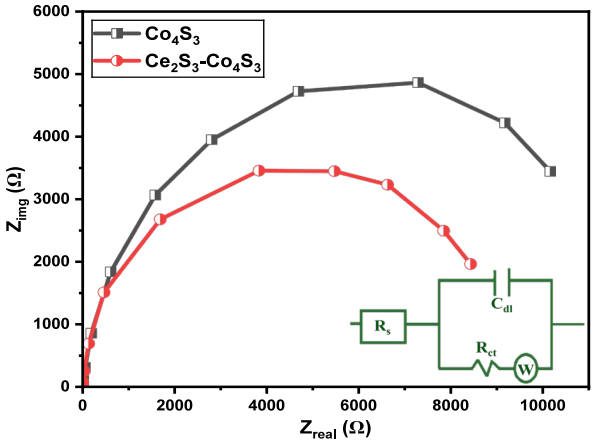

Fig. 6. Electrochemical impedance spectroscopy of pure Co_4S_3 and Ce_2S_3-Co_4S_3 binary composite electrode materials.

4. Conclusion

The pure Co_4S_3 and Ce_2S_3-Co_4S_3 binary nanocomposite materials were investigated for Supercapacitor application and prepared via modified microemulsion mediated hydrothermal

approach. This prepared nanomaterial was confirmed by X-ray diffraction spectroscopy; Fourier transform infrared spectroscopy and scanning electron microscope analysis. The presence of sharp peaks at 857 cm^{-1} and 600 cm^{-1} indicates vibrations of metal -sulfur bonds like Ce-S and Co-S. Similarly, the Ce_2S_3-Co_4S_3 binary composite shows more refined, compact and larger particles structural morphology associated with improved electrochemical analysis. The cyclic voltammetry was assessed for determination of specific capacitance of Co_4S_3 and Ce_2S_3-Co_4S_3 629 and 952 F/g, respectively. The electrochemical impedance spectroscopy showed lower semicircle and improved ions conductivity and fast faradic redox reaction kinetics in Ce_2S_3-Co_4S_3. The high performance of composite material confirms it as a significant material for sustainable energy solutions.

Acknowledgements

The authors would like to acknowledge Deanship of Graduate Studies and Scientific Research, Taif University for funding this work.

Data availability statement

No additional new data were created.

Conflicts of interest

The authors declare that they have no known competing financial interests or personal relationships that could have appeared to influence the work reported in this paper.

References

[1] E. Pomerantseva, F. Bonaccorso, X. Feng, Y. Cui, Y. Gogotsi, Science 366(6468) (2019) eaan8285; https://doi.org/10.1126/science.aan8285

[2] J. Greenspon, G. Hanson, Explorations in Economic History (2025) 101688; https://doi.org/10.1016/j.eeh.2025.101688

[3] M. Gao, W.-K. Wang, X. Zhang, J. Jiang, H.-Q. Yu, The Journal of Physical Chemistry C 122(44) (2018) 25174-25182; https://doi.org/10.1021/acs.jpcc.8b07716

[4] M. Abdel Maksoud, R.A. Fahim, A.E. Shalan, M. Abd Elkodous, S. Olojede, A.I. Osman, C. Farrell, A.a.H. Al-Muhtaseb, A. Awed, A. Ashour, Environmental Chemistry Letters 19(1) (2021) 375-439; https://doi.org/10.1007/s10311-020-01075-w

[5] K.S. Ahmad, S.B. Jaffri, H. Panchal, R.K. Gupta, M.A. Abdel-Maksoud, A. Malik, W.H. Al-Qahtani, New Journal of Chemistry 49(6) (2025) 2291-2307; https://doi.org/10.1039/D4NJ03567D

[6] Y. Jiang, X. Qian, C. Zhu, H. Liu, L. Hou, ACS Applied Materials & Interfaces 10(11) (2018) 9379-9389; https://doi.org/10.1021/acsami.7b18439

[7] S. Rudra, H.W. Seo, S. Sarker, D.M. Kim, Molecules 29(1) (2024) 243; https://doi.org/10.3390/molecules29010243

[8] P. Phogat, S. Sharma, R. Jha, S. Singh, Principles to Applications, Springer2024, pp. 225-255; https://doi.org/10.1007/978-981-96-0527-9_6

[9] U. Evariste, G. Jiang, B. Yu, Y. Liu, Z. Huang, Q. Lu, P. Ma, Journal of Materials Research 34(14) (2019) 2445-2455; https://doi.org/10.1557/jmr.2019.205

[10] C. Jing, X. Guo, L. Xia, Y. Chen, X. Wang, X. Liu, B. Dong, F. Dong, S. Li, Y. Zhang, Chemical Engineering Journal 379 (2020) 122305; https://doi.org/10.1016/j.cej.2019.122305

[11] M.S. Khan, M. Shariq, S.M. Bouzgarrou, R.E. Azooz, S. kashif Ali, W.A. Ghaly, K. Hassan, Physica Scripta 99(6) (2024) 062001; https://doi.org/10.1088/1402-4896/ad3f8a

[12] R. Akram, M.D. Khan, C. Zequine, C. Zhao, R.K. Gupta, M. Akhtar, J. Akhtar, M.A. Malik, N. Revaprasadu, M.H. Bhatti, Materials science in semiconductor processing 109 (2020) 104925; https://doi.org/10.1016/j.mssp.2020.104925

[13] Z.A. Sandhu, M. Danish, U. Farwa, M.A. Raza, A.H. Bhalli, A. Sultan, N. Alwadai, W. Mnif, Journal of Inorganic and Organometallic Polymers and Materials (2025) 1-14; https://doi.org/10.1007/s10904-025-03650-6

[14] K. Hachem, M.J. Ansari, R.O. Saleh, H.H. Kzar, M.E. Al-Gazally, U.S. Altimari, S.A. Hussein, H.T. Mohammed, A.T. Hammid, E. Kianfar, BioNanoScience 12(3) (2022) 1032-1057; https://doi.org/10.1007/s12668-022-00996-w

[15] C. Liu, H. Liu, C. Yin, X. Zhao, B. Liu, X. Li, Y. Li, Y. Liu, Fuel 154 (2015) 88-94; https://doi.org/10.1016/j.fuel.2015.03.034

[16] K. Krishnamoorthy, G.K. Veerasubramani, S.J. Kim, Materials Science in Semiconductor Processing 40 (2015) 781-786; https://doi.org/10.1016/j.mssp.2015.06.070

[17] X. Liang, P. Wang, Y. Gao, H. Huang, F. Tong, Q. Zhang, Z. Wang, Y. Liu, Z. Zheng, Y. Dai, Applied Catalysis B: Environmental 260 (2020) 118151; https://doi.org/10.1016/j.apcatb.2019.118151

[18] F. Wang, X. Li, Y. Qiao, K. Zhou, Z. Li, Synthetic Metals 281 (2021) 116920; https://doi.org/10.1016/j.synthmet.2021.116920

[19] M. Danish, A. Ashraf, Z.A. Sandhu, M.A. Raza, A.H. Bhalli, A.G. Al-Sehemi, Journal of Molecular Structure 1294 (2023) 136296; https://doi.org/10.1016/j.molstruc.2023.136296

[20] X. Cao, J. He, H. Li, L. Kang, X. He, J. Sun, R. Jiang, H. Xu, Z. Lei, Z.H. Liu, Small 14(27) (2018) 1800998; https://doi.org/10.1002/smll.201800998

[21] A.Y. Ahmed, A.K. Ogundele, M.S. Hamed, N.A. Tegegne, A. Kumar, G. Sharma, G.T. Mola, Materials Science in Semiconductor Processing 185 (2025) 108917; https://doi.org/10.1016/j.mssp.2024.108917

[22] T. Abza, D.G. Dadi, F.G. Hone, T.C. Meharu, G. Tekle, E.B. Abebe, K.S. Ahmed, Advances in Materials Science and Engineering 2020(1) (2020) 2628706; https://doi.org/10.1155/2020/2628706

[23] S. Nandhini, G. Muralidharan, Journal of Materials Science 57(10) (2022) 5933-5953; https://doi.org/10.1007/s10853-022-06987-2

[24] N. Kandhasamy, G. Murugadoss, T. Kannappan, K. Kirubaharan, R.K. Manavalan, R. Gopal, Environmental Science and Pollution Research 30(11) (2023) 29711-29726; https://doi.org/10.1007/s11356-022-24311-y

[25] S. Sibokoza, M. Moloto, N. Moloto, P. Sibiya, Chalcogenide Letters 14(2) (2017)

[26] M. Zahid, N. Yasmin, M.N. Ashiq, M. Safdar, M. Mirza, Physica B: Condensed Matter 624 (2022) 413359; https://doi.org/10.1016/j.physb.2021.413359

[27] D. Yu, F. Zhang, Y. Zhang, M. Tian, H. Lin, W. Guo, F. Qu, ACS Applied Energy Materials 6(11) (2023) 6348-6356; https://doi.org/10.1021/acsaem.3c00940

[28] H. Gao, Z. Xu, S. Lin, Y. Sun, L. Li, Langmuir 40(40) (2024) 21077-21085; https://doi.org/10.1021/acs.langmuir.4c02475

[29] S.A. Bhat, A.M. Tantray, J.U. Ahsan, M. Ikram, Ceramics International 50(14) (2024) 26220-26233; https://doi.org/10.1016/j.ceramint.2024.08.283

[30] S. Khasim, A. Pasha, B. Ramakrishna, P. BS, Materials Chemistry and Physics 325 (2024) 129675; https://doi.org/10.2139/ssrn.4791329

[31] P.N. Nikam, S.S. Patil, U.M. Chougale, A.V. Fulari, V.J. Fulari, Journal of Energy Storage 96 (2024) 112648; https://doi.org/10.1016/j.est.2024.112648

[32] S. Ashraf, Z.A. Sandhu, M.A. Raza, A.H. Bhalli, M. Hamayun, A. Ashraf, A.G. Al-Sehemi, Un Journal of Sol-Gel Science and Technology 112(1) (2024) 25-43; https://doi.org/10.1007/s10971-024-06500-y